Proceedings of the 37th IEEE
Conference on Decision & Control
Tampa, Florida USA • December 1998

Adaptive Eccentricity Compensation

Carlos Canudas de Wit and Laurent Praly

Laboratoire d'Automatique de Grenoble, UMR CNRS 5528
ENSIEG-INPG, BP 46, 38402, ST. Martin d'Hères, France
canudas@lag.ensieg.inpg.fr

Ecole des mines de Paris, Centre Automatique
35, rue Saint-Honoré, 77305 Fontainebleau France.
praly@cas.ensmp.fr

Abstract

This paper is devoted to the problem of rejecting oscillatory position-dependent disturbances (eccentricity) with unknown frequency and unknown amplitude. Most of the previous works on eccentricity cancellation assume a *time-depending* oscillation, we instead assume that the oscillatory disturbance is position-dependent. This leads us to formulate and to globally solve the adaptive cancellation problem in the spatial domain coordinates (curvilinear abscissa associated to the trajectory of the motion), which is the *rate-independent* (or space) description of the position. An apparatus with rolling excentricity has been build to test the controller.

Keywords: Adaptive compensation, Eccentricity sinusoidal disturbance rejection.

1. Introduction

We consider systems of the form:

$$J\dot{v} = u + d(x); \quad v = \dot{x} = \frac{dx}{dt} \tag{1}$$

where x is the system angular position, J is the inertia, u is the control input and $d(x)$ is the position-dependent oscillatory disturbance defined as:

$$\begin{aligned} d(x) &= \Lambda \cos(\omega x + \Phi) && (2)\\ &= a_1 \cos \omega x + a_2 \sin \omega x && (3) \end{aligned}$$

It is assumed that the amplitude Λ, the dimensionless frequency ω, and the phase Φ (or equivalent, the parameters (a_1, a_2, ω)), of the disturbance d, are unknown. The problem considered here is thus to cancel the effect of the disturbance d in the system (1).

This type of problem arises as a consequence of eccentricity in many mechanical systems where the center of rotation does not correspods with its geometric center. This is typically the case on drives with magnetic bearings. It also arrises in systems with friction where the contact forces change as a function of the position x.

The dependency on position of $d(x)$ can be visualized in the following scenarios. It is known that the friction forces depends on the normal force acting between two surfaces. Inaccuracies in the geometric position of the rotating axis of a rolling mill (eccentricity), will produce position dependent disturbances. In gear boxes, friction will vary as a function of the effective surface in contact of the gear's teeth. The two dimensional rolling and spinning friction causes in ball bearings the frictional torque to be dependent on both position and velocity. Figure (1) shown some of these examples.

Many of the existing works consider d not as a position function, but as a time-dependent exogenous signal, of the form

$$d(t) = \Lambda \cos(\omega t + \Phi) \tag{4}$$

In the previous mentioned system this hypothesis is only valid if we assume that the system is operating and regulated, at constant velocity $v_d$so that $x(t)$ becomes proportional $t \cdot v_d$. Disturbances of the form (4) have been considered in problems such as active noise and vibration control. The noise $d(t)$ is thus assumed to be generated by the rotating machinery and transmitted through the sensor path. Examples rate from engine noise in turboprop aircraft [7] to ventilation noise in HVAC system [8], passing through engine noise in automobiles [12].

The proposed solutions resort to "standard" adaptive algorithms if the frequency ω is assumed to be known [4]. Repetitive control has also been used to compensate eccentricity in rolling [9]. For the general case where both amplitude and frequency are unknown, some approaches based on the *phase-lock loop* principle has been proposed [3], but without proof of stability. When formulating this problem in the time-domain, the main difficulty to show global stability properties of the adaptive algorithms comes from the fact that the unknown parameters appear

0-7803-4394-8/98 $10.00 © 1998 IEEE

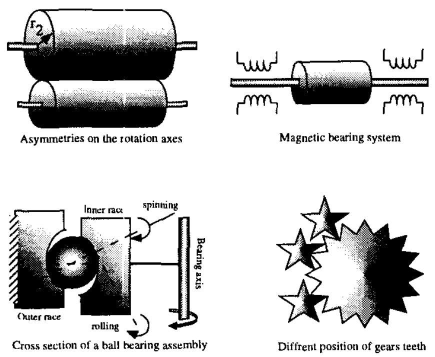

Figure 1: Examples of systems where disturbances $d(x)$ are positions-dependent.

nonlinearly in the expression of (4).

When the system operates under time-varying velocity profiles, ω in (4) becomes time-dependent generating a signal $d(t)$ with a large spectral support. The position dependent disturbance model (3) is thus better adapted for those cases.

In this paper we present a globally stable adaptive algorithm that solves the above mentioned problem. For this, we use a formulation in the in the s-domain (curvilinear abscissa associated to the trajectory of the relative motion), which is the *rate-independent* (or space) description of the position. An internal model and adaptive observer are thus designed in the s-domain, and global stability is thus demonstrated.

2. Spatial transformation

In this section we introduce the the s-domain operator ∇, we formulate the internal model for the disturbance d in this coordinates, and we present some useful properties required to establish our stability results in the following section.

Definition of the ∇-operator Introduce first the spatial variable s, as being the curvilinear abscissa associated to the trajectory of the relative motion:

$$s(t) \triangleq \int_0^t |v(\tau)| d\tau \tag{5}$$

$s(t)$ is a monotonous growing signal.

Let ∇ be defined as:

$$\nabla \triangleq \frac{d}{ds} = \frac{1}{|v|} D \tag{6}$$

where $D \triangleq \frac{d}{dt}$ stands for the time-differential operator. Since ∇ is a derivation, similar rules that apply for D can be used for ∇. In particular if x and y are two functions, we have

$$\nabla(xy) = \nabla(x)y + x\nabla(y) \ . \tag{7}$$

Also to any differential equation in the s-domain

$$\nabla x = f(x) \tag{8}$$

it corresponds a non autonomous differential equation in the t-domain, i.e.

$$Dx = \dot{x} = |v(t)| f(x) \ . \tag{9}$$

The converse may not hold in general with a problem when $v(t) = 0$.

This type of transformation has been used before in connection with hysteresis operators (see [10], [13]), and more recently as a mathematical tool to model dynamic friction [2]. In particular, authors in [2] and [1] shown how the nonlinear Dahl's friction model can be transformed into a linear spatial invariant system.

Internal ∇-model for d. Let

$$y \triangleq J\dot{v} - u = d(x) \tag{10}$$

with $d(x)$ given in (3). Computation of ∇y and $\nabla^2 y$, gives:

$$\begin{aligned} \begin{pmatrix} y \\ \nabla y/\omega \end{pmatrix} &= \begin{pmatrix} \cos\omega x & \sin\omega x \\ -\sin\omega x & \cos\omega x \end{pmatrix} \begin{pmatrix} a_1 \\ a_2 \end{pmatrix} && (11) \\ \nabla^2 y &= -\omega^2 y && (12) \end{aligned}$$

where the equation (12) describes the internal model for y. Let $z_1 = y$, and $z_2 = \nabla y$, a s-domain state space realization for (12) is:

$$\begin{aligned} \nabla z &= \begin{pmatrix} 0 & 1 \\ -\theta & 0 \end{pmatrix} z && (13) \\ y &= (1, 0) z && (14) \end{aligned}$$

with $\theta = b^2$, and $z = [z_1, z_2]^T$.

3. Control design

In this section the control law, the adaptive observer, and the adaptation law will be presented. Stability is studied at the end of the section. The control design philosophy consists in first designing an adaptive internal model predictor for d, directly in the s-domain, and then to study the stability properties of the coupled s-domain and t-domain equations.

We consider the problem of tracking the desired velocity $v_d(t)$ supposed to be bounded and continuous (for simplicity) as well as its derivative. To this aim we define the adaptive eccentricity control (AEC) control as:

$$u = J\dot{v}_d - k_v(v - v_d) - \hat{z}_1, \tag{15}$$

where $\hat{z}_1$ is an output of the following dynamic system (observer):

$$\begin{aligned} \nabla \hat{z}_1 &= \hat{z}_2 + k_1(z_1 - \hat{z}_1) && (16) \\ \nabla \hat{z}_2 &= -\hat{\theta}\hat{z}_1 + k_2(z_1 - \hat{z}_1) - \lambda \bar{z}_1 \nabla \hat{\theta} && (17) \\ \nabla \bar{z}_1 &= -\frac{1}{\lambda}(\mu \bar{z}_1 - \hat{z}_1) && (18) \\ \nabla \hat{\theta} &= -\gamma \bar{z}_1 (z_1 - \hat{z}_1) && (19) \end{aligned}$$

with

$$y = z_1 = J\dot{v} - u = a_1 \cos(\omega x) + a_2 \sin(\omega x) \qquad (20)$$

and positive nonzero constants $k_v, k_1, k_2, \lambda, \mu$, and γ. As we shall see this representation of the controller is appropriate for analysis. But it cannot be implemented directly in this way unless the system acceleration, is assumed to be measurable. Alternatively, we can first transform the system (16)-(19) to the time-domain, and then show that measurement of $\dot{v}$ is not needed. For the former, we have readily

$$\begin{aligned} \dot{\hat{z}}_1 &= |v| \left[\hat{z}_2 + k_1(J\dot{v} - u - \hat{z}_1)\right] && (21)\\ \dot{\hat{z}}_2 &= |v| \left[-\hat{\theta}\hat{z}_1 + k_2(J\dot{v} - u - \hat{z}_1) - \lambda \bar{z}_1 \nabla \hat{\theta}\right] && (22)\\ \dot{\bar{z}}_1 &= |v| \left[-\frac{1}{\lambda}(\mu \bar{z}_1 - \hat{z}_1)\right] && (23)\\ \dot{\hat{\theta}} &= |v| \left[-\gamma \bar{z}_1 (J\dot{v} - u - \hat{z}_1)\right] && (24) \end{aligned}$$

For the latter, noting that

$$\frac{d}{dt}\left\{|v|\, v^i\right\} = (i+1)\,|v| v^{i-1}\, \dot{v} \quad \forall i = 1, 2, 3, \ldots \qquad (25)$$

and introducing

$$\begin{aligned} \hat{\zeta}_1 &= \hat{z}_1 - \frac{k_1 J}{2}|v|v && (26)\\ \hat{\zeta}_2 &= \hat{z}_2 - \frac{k_2 J}{2}|v|v - \frac{\gamma\lambda J}{2}|v|v\bar{z}_1^2 && (27)\\ \bar{\zeta}_1 &= \bar{z}_1 && (28)\\ \hat{\vartheta} &= \hat{\theta} + \frac{\gamma J}{2}\bar{z}_1|v|v && (29) \end{aligned}$$

We have

$$\begin{aligned} \dot{\hat{\zeta}}_1 &= |v| \left[\hat{z}_2 - k_1(u + \hat{z}_1)\right] && (30)\\ \dot{\hat{\zeta}}_2 &= |v| \Big[-(k_2 + \hat{\theta})\hat{z}_1 - k_2 u - \gamma\lambda \bar{z}_1^2 (u + \hat{z}_1) \\ &\quad + \gamma J |v| v \bar{z}_1 (\mu \bar{z}_1 - \hat{z}_1)\Big] && (31)\\ \dot{\bar{\zeta}}_1 &= |v| \left[-\frac{1}{\lambda}(\mu \bar{z}_1 - \hat{z}_1)\right] && (32)\\ \dot{\hat{\vartheta}} &= |v| \left[\gamma \bar{z}_1 (u + \hat{z}_1) - \frac{\gamma J}{2\lambda}|v|v(\mu \bar{z}_1 - \hat{z}_1)\right] && (33) \end{aligned}$$

This gives us a well defined t-domain state space realization depending only on the measurable velocity v . Note that with the assumption that $\dot{v}_d$ and v_d are bounded and continuous, with this controller, we get a closed loop system whose dynamics are described by an ordinary differential equation whose right hand side is continuous.

To analyze this closed-loop system, we introduce the error variables:

$$e = v - v_d, \quad \tilde{z} = z - \hat{z}, \quad \tilde{\theta} = \theta - \hat{\theta} \; .$$

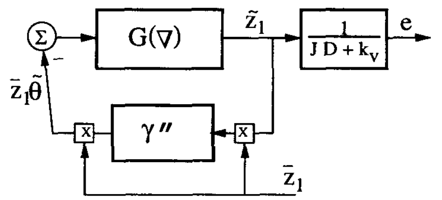

Figure 2: Block scheme of the coupled s-domain / t-domain error system.

After doing some simple manipulations, the coupled s-domain / t-domain error equations are given by:

$$\begin{aligned} J\dot{e} &= -k_v e + \tilde{z}_1 && (34)\\ \tilde{z}_1 &= G(\nabla)\left\{-\bar{z}_1\tilde{\theta}\right\} && (35)\\ \nabla\tilde{\theta} &= \gamma \bar{z}_1(\tilde{z}_1) && (36) \end{aligned}$$

with the map $G(\nabla)$ defined as:

$$G(\nabla) = \frac{\lambda\nabla + \mu}{\nabla^2 + k_1 \nabla + (k_2 + \theta)} \qquad (37)$$

Figure 2 shows the inter-block connection among these systems. Note that the closed-loop block interconnection, at the left of the figure –Equations (38-36)– involves signals that are parameterized in the t-domain, whereas the block at the right –Equation (34)– involves a LTI map having as input a signal parameterized in s. This results in a coupled s-domain / t-domain system.

Stability analysis Note that the map $G(\nabla)$ admits a state space representation of the form:

$$\begin{aligned} \nabla\xi &= A\xi - B\bar{z}_1\tilde{\theta} && (38)\\ \tilde{z}_1 &= C\xi && (39) \end{aligned}$$

where:

$$A = \begin{pmatrix} 0 & 1 \\ -(k_2+\theta) & -k_1 \end{pmatrix}, B = \begin{pmatrix} 0 \\ 1 \end{pmatrix}, C^T = \begin{pmatrix} \lambda \\ \mu \end{pmatrix} \qquad (40)$$

and $\xi = T\tilde{z}$, for some invertible linear transformation T. Since A in (40) is strictly Hurwitz for any positive value of k_2 (note that $\theta > 0$), and k_1, it follows that we can find P symmetric positive definite matrix such that:

$$A^T P + P A = -I \; . \qquad (41)$$

Then let λ and μ in C in (40) be defined as:

$$C = PB \; . \qquad (42)$$

Theorem 1 *Consider the system (1)-(3). Consider the dynamic feedback defined by the equation set (15- 19). Let the control gains $k_1 > 0, k_2 > 0$, and λ, μ be defined by (42). Then all the internal signal of the system are bounded and in addition, the velocity tracking error e tends* *to zero, if the desired velocity time-profile is rich enough to meet*

$$\liminf_{t\to+\infty} \frac{1}{t}\int_0^t |v_d(\tau)|d\tau = +\infty$$

else, $v - v_d$ tends to some finite value.

Proof: From what we have observed on the closed loop system, to any initial condition corresponds a unique solution. Let $[0, T)$ be its right maximal in terval of definition in the t-domain. It corresponds functions in the s-domain defined on an interval $[0, S_{max})$ where:

$$S_{max} = \lim_{t\to T}\int_0^t |v(\tau)|d\tau \ (\leq +\infty) \tag{43}$$

Let us show that T must be infinite. To do this we consider the non negative function V:

$$V = \xi^T P\xi + \gamma^{-1}\tilde{\theta}^2$$

with P given in (41). With the help of (38)-(39), (36), (41) and (42), we obtain in the s-domain:

$$\begin{aligned}
\nabla V &= -\xi^T\xi - 2(\xi^T PB)\tilde{z}_1\tilde{\theta} + \gamma^{-1}(\nabla\tilde{\theta})\tilde{\theta} && (44)\\
&= -\xi^T\xi - 2\tilde{z}_1\bar{z}_1\tilde{\theta} - \gamma^{-1}(\nabla\hat{\theta})\tilde{\theta} && (45)\\
&= -\xi^T\xi - 2\left[\tilde{z}_1\bar{z}_1 + \gamma^{-1}\nabla\hat{\theta}\right]\tilde{\theta} && (46)\\
&= -\xi^T\xi && (47)
\end{aligned}$$

where Equation (46) results from the adaptation law that cancels the terms in the square brackets in (45) (this is how its is designed). Since ∇V is non positive, V it is bounded on $[0, S_{max})$ and therefore on $[0, T)$ it follows that ξ, $\tilde{z}_1$ and $\hat{\theta}$ are bounded on $[0, T)$. But from (34), the same holds for e. Since the external signals $\dot{v}_d$, v_d and z_1 (see (20)) are bounded, we conclude that all the functions are bounded. So T must be infinity.

From (47), we have also

$$\int_0^s \xi(\tau)^T\xi(\tau)d\tau \ \leq \ V(0) \qquad \forall s \in [0, S_{max}) \tag{48}$$

Since from (38), $\nabla\xi$ is bounded on $[0, S_{max})$ and ξ is uniformly continuous. From Barbalat's Lemma, this implies that, if $S_{max} = \infty$, i.e. $|v|$ is not summable in the time domain, then ξ and therefore $\tilde{z}_1$ converge to 0 as t goes to infinity. From (34), the same holds for e. So when $|v|$ is not summable in the time domain, we have:

$$\lim_{t\to+\infty}\{v(t) - v_d(t)\} = 0 \ . \tag{49}$$

When S_{max} is finite, i.e. $|v|$ is summable on $[0, \infty)$, from (21) and the boundedness of the functions, we have that $\dot{\tilde{z}}_1$ is summable on $[0, +\infty)$. This implies the existence of $\tilde{z}_{1\infty}$ such that

$$\lim_{t\to+\infty}\tilde{z}_1(t) \ = \ \tilde{z}_{1\infty} \tag{50}$$

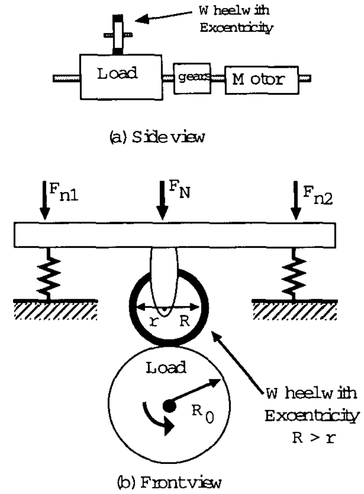

Figure 3: Schematic (a) front view of the experimental setup to study eccentricity, (b) lateral view.

So again from (34), we get the existence of e_∞ such that

$$\lim_{t\to+\infty}\{v(t) - v_d(t)\} = \ e_\infty \ . \tag{51}$$

Note that this implies by contradiction that if v_d is such that:

$$\liminf_{t\to+\infty} \frac{1}{t}\int_0^t |v_d(\tau)|d\tau = +\infty \tag{52}$$

$|v|$ cannot be summable and therefore (49) holds. ∎

4. Experimental results

This section describes the experimental evaluation of AEC-controller. More detailed description of the real-time system used for these experiments, as well as additional experiments, can be found in [11].

The schematic view of the aparatus build to study eccentricity is shown in Fig 3. The load cylinder of inertia J_l is driven by the motor of inertia J_m. On the top of it, we have placed a rotating wheel (with neglected inertia), constrained by the force F_N. The rotation wheel's center is set to be different to its geometric center. The contact pressure at the point where the wheel radius is equal to R, is larger than the contact pleasure at the point of radius r, since $R > r$. This produces an eccentricity effect changing the normal force acting on the wheel-to-cylinder contact surface.

The model for the motor drive under this setup is given as:

$$J\dot{v} = u - F - \Lambda\cos(\omega x + \Phi) \tag{53}$$

with:

$$\begin{aligned}
F &= \sigma_0\eta + \sigma_1\dot{\eta} + \sigma_2 v && (54)\\
\dot{\eta} &= v - \frac{\sigma_0|v|}{F_C}\eta; \quad F_C \triangleq \mu_0(\frac{F_N}{n} + F_{Nm}) && (55)
\end{aligned}$$

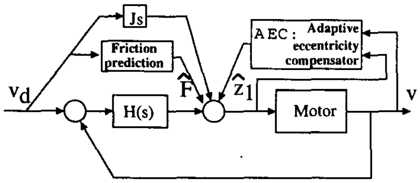

Figure 4: Control block scheme of the adaptive eccentricity compensator (AEC), with feedforward friction compensation.

$$\omega = \frac{\bar{\omega}}{n} = \frac{2R_0}{n(r+R)} \qquad (56)$$

$$\Lambda = \frac{R-r}{2}\cdot\frac{F_N}{n}\nu(\eta,\dot{\eta},v) \qquad (57)$$

$$\approx \frac{R-r}{2}\cdot\frac{F_N}{n}\nu_{SS} = \frac{R-r}{2}\cdot\frac{F_N}{n}\mu_0\cdot\mathrm{sign}(v) \qquad (58)$$

where F_{Nm} is the average normal force on the ball bearings, the parameters σ_i are the friction parameters associated to the LuGre friction model (see [5]). F_C is the Coulomb friction. The Stribeck effect has been neglected. They capture the distributed friction characteristics on the motor. ω is the dimensionless frequency at the motor side (note that the eccentricity frequency effect at the motor shaft is demultiplied by the gear ratio n).

The model (53), differs from model (1) by the presence of friction, and by the dependence of Λ on the normalized velocity dependent friction $\nu(\cdot) \triangleq F(\cdot)/F_{max}$. Hence to apply to our previous adaptive eccentricity compensator, we need to cancel the friction, and to assume that $\nu(\eta,\dot{\eta},v)$, can be approximate by its steady state value $\nu_{SS} = \mu_0 \mathrm{sign}(v)$, as shown in (58).

Friction can be cancelled via feedforward or feedback. The approximation on $\nu(\cdot)$ may hold for most operation conditions (except for the time periods when the velocity crosses zero) since the friction dynamics of (55), is much more faster that the motor velocity dynamic (of the order of magnitude of σ_0). The only conceptual problem lies thus on the velocity zero crossings that occurs at isolated time periods.

System parameters including friction coefficients has been estimated using a similar procedure as described in [6]. They are reported in the table below.

Friction parameters	Motor parameters	Wheel & cylinder characteristics
$F_C = 0.38$ $[Nm]$	$J_m = 0.00196$ $[Kg/m^2]$	$R_0 = 6$ $[cm]$
$F_S = 0.42$ $[Nm]$	$J_l = 0.0125$ $[Kg/m^2]$	$R = 2.1$ $[cm]$
$v_0 = 0.01$ $[rad/sec]$	$J = 0.0022$ $[Kg/m^2]$	$r = 1.9 [cm]$
$\sigma_0 = 260.0$ $[Nmsec/rad]$	$K_t = 0.352$ $[Nm/Amp]$	
$\sigma_1 = 0.6$ $[Nm/rad]$	$n = 15.5$	
$\sigma_2 = 0.011$ $[Nmsec/rad]$	Power $= 200$ $[Wats]$	

Table 1: Motor, friction, and load parameters.

The AEC controller, with feedforward compensation is:

$$u = J\dot{v}_d - k_v(v - v_d) + \hat{F} - \hat{z}_1, \qquad (59)$$

where $\hat{z}_1$ is given by the set of equations (27)-(33), and $\hat{F}$ is a feedforward friction prediction obtained from the equations:

$$\hat{F} = \sigma_0\hat{\eta} + \sigma_1\dot{\hat{\eta}} + \sigma_2 v_d \qquad (60)$$

$$\dot{\hat{\eta}} = v_d - \frac{\sigma_0|v_d|}{\mu_0}\hat{\eta}, \quad \hat{\eta}(0) = 0. \qquad (61)$$

Figure 4, shown the block diagram of the AEC control scheme with feedforward friction compensation. Locally, $\hat{F} \approx F$, thus the closed-loop equation with this additional friction compensation term is similar to the frictionless system studied in the previous section.

The control parameters used for these experiments were: $k_v = 40$, $k_1 = 1$, $k_2 = 0.25$, $\gamma = 2$, $\lambda = 2$, $\mu = 1$.

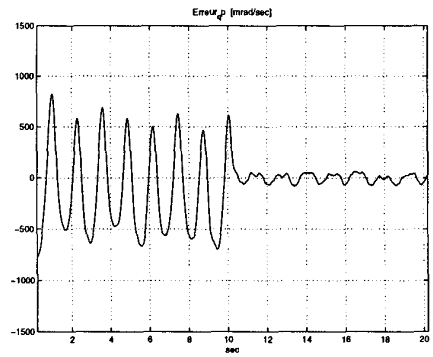

Figure 5: Velocity tracking error ($v_d - v$)

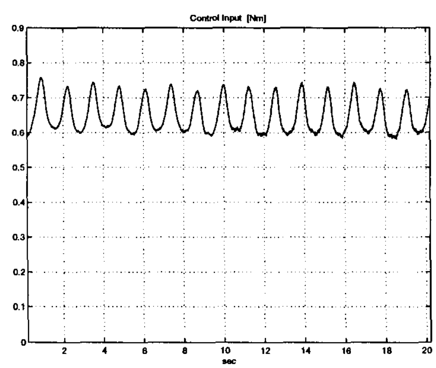

Figure 6: control input time profile.

The experiments in Figures 5-8, show the tracking error, the prediction $\hat{z}_1(t)$, the estimate $\hat{\theta}$, and the control signal. The experiments are realized at $v_d = 30$ Rad/sec. The eccentricity compensation is applied at $t = 10sec$. It can be observed that the oscillatory disturbance affecting the tracking error is canceled when applying the term $\hat{z}_1(t)$, in u. The remaining error, which is about 12% of v_d before compensation, is reduced to 1.5% with the compensation. The time-profiles shown in all the presented figures has been filtrate for improve their visibility.

The time evolution of $\hat{z}_1(t)$, has a shape similar to a sinusoidal wave (as it has been predicted). The imperfections may be attributed to the nonuniform deformation

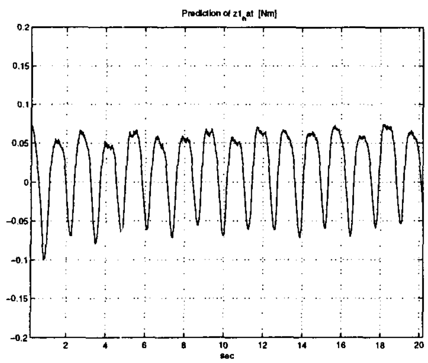

Figure 7: predicted disturbance, $\hat{z}_1$

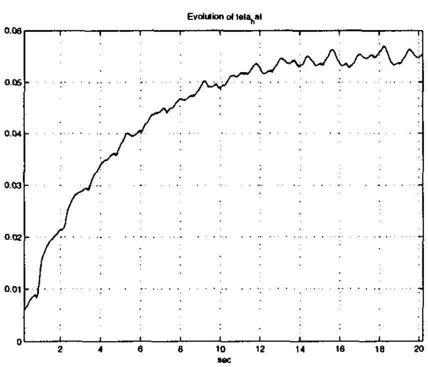

Figure 8: Time-evolution of $\hat{\theta}(t)$

of the wheel contact surface (the wheel in contact is composed of a inner undeformable steel wheel, covered by a rubber $5mm$ o-ring). The estimated parameter $\hat{\theta}$ is observed to converge (in average sense) to a value close to 0.055, which according to (3) implies that $\omega = \sqrt{0.055} = 0.23$. The theoretical value of ω is given by the expression 56 as $\omega = \frac{2R_0}{n(r+R)} = 3/15 = 0.2$, which seems to correspond to the experimental found value (note also that the period of $\hat{z}_1(t)$ gives for a velocity of $30 Rad/sec$, an experimental value of $\omega = (2\pi)/(vT) \approx 0.2$, for a $T = 1.6\pi$).

5. Conclusions

We presented a method for compensating eccentricity in mechanical system. As a main difference with previous works, we have formulated the disturbance as a position-dependent periodic function. This formulation seems to be justified in most of the mechanical applications where eccentricity occurs.

As a results of this formulation, we have used a spatial description of the system (often used in system with hysteresis) which is more natural than the use of a time formulation. This did allows us to design of an adaptive predictor of the disturbance directly in the spatial domain. Experiments shown that the AEC controller improves over simpler linear controller without eccentricity compensation.

6. Acknowledgements

The first author would like to thanks Petra Posselius, and Holger Olofsson, for the help in performing the experiments, and the interesting discussion that results during their stay at Grenoble.

References

[1] Bliman, P.A. (1992), "Mathematical study of the Dahl's friction model" *European Journal of Mechanics, A./Solid.*, Vol. 11, No6, 1992.

[2] Bliman, P.A., and M. Sorine (1997), "Friction modeling by hysteresis operator. Application to Dahl, sticktion and Stribeck effects" *private correspondence.*

[3] Bodson, M. and S.C. Douglas (1997), "Adaptive algorithm for the rejection of periodic disturbances with unknown frequency" *Automatica*,Vol. 33, No. 12, pp.2213-2221, 1997.

[4] Bodson, M., A. Sacks and P. Khosla (1994), "Harmonic generation in adaptive feedforward cancellation schemes" *IEEE Trans. Automat. Control*, **39**(9), 1939-1944.

[5] Canudas de Wit, C., H. Olsson, K.J. Åström, and P. Lischinsky, (March, 1995), "A New Model for Control of Systems with Friction", IEEE TAC, Vol. 40, No. 3, pp.419-425.

[6] Canudas de Wit, and P. Lischinsky, (1997), "Adaptive friction compesnation with partially known dynamic friction model", International Journal of Adaptive Control and Signal Processing, Vol. 11, pp.65-85 (1997).

[7] Emborg, U. and C.F. Ross (1993), "Active control in the Saab" *340. Proc. 2nd Conf. Recent Adv. Active Control Sound Vibrations*, Blacksburg, VA pp S67-S73.

[8] Eriksson, L. J. (1988), "A practical system for active attenuation in ducts" *Sound and Vibration*, **22**(2), 30-40.

[9] Garimella, S. S., and K. Srinivasan (1996), "Application of repetitive control to eccentricity compensation in rolling" *Journal of Dynamic Systems, Measurement and Control*, Dec. 1996, Vol. 118, pp. 657-664.

[10] Krasnolesl'skii, M.A., and A.V. Pokrovskii (1989), *Systems with hysteresis*, Springer-Verlag, 1989.

[11] Olofsson, H. , and P. Posselius (1998), "Experimental study of adaptive eccentricity compensation". *Internal report. Automatic Control Departement of Grenoble, Sept. 1998*

[12] Shoureshi, R. and P. Knurek (1996), "Automotive application of a hybrid active noise and vibration control" *IEEEE Control systems*, **16**(6), 72-78.

[13] Visintin, A. (1988), *Mathematical models of hysteresis*, Topics in nonsmooth analysis, Birkhaser Verlag, 295-326, 1988.